Journal Name

Dynamic Article Links ►

Cite this: DOI: 10.1039/c0xx00000x

www.rsc.org/xxxxxx

ARTICLE TYPE

Effects of Natural Organic Matter Type and Concentration on the Aggregation of Citrate-Stabilized Gold Nanoparticles

Jeffrey A. Nason,*[a] Shannon A. McDowell‡[a] and Ty W. Callahan[b]

Received (in XXX, XXX) Xth XXXXXXXXX 20XX, Accepted Xth XXXXXXXXX 20XX

DOI: 10.1039/b000000x

The aggregation of 12 nm citrate-stabilized gold nanoparticles (cit-AuNPs) in the presence of four different natural organic matter (NOM) isolates and a monovalent electrolyte (KCl) was evaluated using time-resolved dynamic light scattering. All four NOM isolates stabilized the cit-AuNPs with respect to aggregation. However, specific effects varied among the different NOM isolates. At pH = 6 in 80 mM KCl, low concentrations (<0.25 mg C/L) of large molecular weight Suwannee River Humic Acid (SRHA) was required to stabilize cit-AuNPs, while larger concentrations (>2 mg C/L) of smaller Suwannee River Fulvic Acid (SRFA) were necessary at the same ionic strength. Suwannee River NOM (SRNOM) which contains both SRHA and SRFA behaved in a manner intermediate between the two. Pony Lake Fulvic Acid (PLFA), an autochthonous NOM isolate, provided substantial stability at low concentrations, yet aggregation was induced at NOM concentrations > 2 mg C/L, a trend that is hypothesized to be the result of favourable hydrophobic interactions between coated particles induced at increased surface coverage. For all NOM isolates, it appears that NOM adsorption or conformational changes at the AuNP surfaces result in significant increases in the hydrodynamic diameter that aren't attributable to NP-NP aggregation.

Introduction

New classes of engineered nanomaterials are rapidly being developed and incorporated into consumer goods.[1] Yet, the environmental implications of the potential release of these novel materials into the environment through their manufacture, distribution, use and disposal are largely unknown.[2, 3] It is imperative that the continued development of materials in this booming field be paralleled with detailed study of the environmental implications, including a focus on environmental transport, transformations and fate. The objective of this research was to investigate the roles that natural organic matter (NOM) type and concentration play in influencing the colloidal stability of one class of engineered nanomaterial, citrate-stabilized gold nanoparticles (cit-AuNPs).

It is well established that the adsorption of NOM to the surfaces of natural colloids[4-6] and engineered nanoparticles (ENPs)[7-14] influences, and often controls, surface properties and colloidal stability in natural aquatic systems. Operating in much the same manner, capping agents (charged species, organic ligands, and polymers) are commonly used to tailor nanoparticle properties (*e.g.*, solubility, chemical reactivity, surface chemistry, binding affinity, and colloidal stability). In many instances, the effects of mono- and divalent ions and pH on the stability of ENPs are observed to follow Derjaguin-Landau-Verwey-Overbeek (DLVO) theory where particle stability is controlled by total interaction energy, typically consisting of repulsive electrostatic interactions between like charged particles and attractive van der Waals forces.[15] However, in the presence of NOM and other stabilizing agents, non-DLVO forces including hydrogen bonding, hydration pressure, Lewis acid base interactions, and steric interactions, are also important but not as well understood.[15-17] Various authors have attributed the stability of NOM coated particles (natural or engineered) to enhanced electrostatic[14, 18] and steric[6-8, 14, 19] effects imparted by the NOM coating. In other instances, bridging flocculation of natural colloids and engineered nanoparticles has been seen in presence of NOM[6, 8, 20] and exacerbated when elevated concentrations of divalent cations are present.[7, 21]

A crucial step in the evaluation of NP transport, transformation, toxicity and fate in the environment is a systematic analysis of factors controlling the interactions between NOM and ENPs. Many of the studies cited above have used a single NOM isolate such as Suwannee River Humic Acid (SRHA) to represent NOM. Although tremendously useful as a standardized material, in reality, the character and concentration of NOM can vary substantially in different aquatic systems. Systematic investigations of the influences of different NOM fractions or NOM from different sources are lacking, although a few recent studies have examined ENP stability in the presence of different NOM isolates[19] or actual water samples.[11, 22, 23] As a result, much remains unknown about (1) what characteristics of NOM influence their interactions with engineered nanoparticles; (2) the influence of NOM concentration; and (3) the mechanisms by which NOM interacts with ENPs (coated and uncoated) and

what implications those interactions have for ENP colloidal stability in aquatic systems.

A large body of work indicates that interactions between NOM and ENPs in aquatic systems influence surface chemistry and stability and that those interactions will also influence environmental transport and fate. However, the current paradigm for assessing environmental behavior appears to be a process of testing materials and release scenarios (*e.g.*, dispersion in different aquatic chemistries) one by one. There is a need to take a broader view that will correlate environmental behavior with specific properties of the ENPs and the aquatic chemical composition (including NOM content and character) and to incorporate those findings into predictive models for environmental transport and fate.

In this article, we present the results of time-resolved dynamic light scattering experiments used to quantify the rates of aggregation of cit-AuNPs as a function of ionic strength in the presence and absence of varying concentrations of four different NOM isolates. We discuss the correlation of cit-AuNP aggregation behavior with the physicochemical properties of the different NOM isolates, as well as reporting on the influence of NOM concentration. Additionally, we discuss the results of supporting analyses using small-angle x-ray scattering to shed light on the mechanisms of the NOM-NP interactions.

Materials and methods

Gold nanoparticles

Citrate-stabilized gold nanoparticles (cit-AuNPs) (NanoXact) were purchased from NanoComposix, Inc. (San Diego, CA). As measured by TEM and reported by the manufacturer, AuNP core diameter was 12.0 ± 1.3 nm (1 standard deviation). The average hydrodynamic diameter as measured by dynamic light scattering in distilled deionized (DDI) water was 20.2 ± 3.1 nm (95% CI, n = 10). The difference in the two methods may be partly attributed to the layer of adsorbed citrate ions, although several reports of citrate adsorption onto gold and gold colloids suggest an adsorbed layer thickness on the order of 0.4-0.7 nm[24, 25], not large enough to account for the differences seen here. Another possible explanation is that the NPs were slightly aggregated in the stock solution.

Natural organic matter isolates

Suwannee River Natural Organic Matter (SRNOM), Suwannee River Humic Acid (SRHA), Suwannee River Fulvic Acid (SRFA), and Pony Lake Fulvic Acid (PLFA) were purchased from the International Humic Substance Society (IHSS). Each NOM isolate was dissolved to a concentration of approximately 40 mg/L total organic carbon (TOC) in distilled deionized (DDI) water (Barnstead Nanopure). The NOM solutions were stirred for 24 hr in the dark and then filtered through a 0.2 µm nylon membrane syringe filter (Whatman). The pH of the stock solutions was adjusted to 6.0 with NaOH or HCl as appropriate. Final dissolved organic carbon concentrations of the stock solutions were quantified using a Shimadzu TOC-VCSH total organic carbon analyzer (EPA Method 415.1).

Electrolytes

All inorganic salts were ACS reagent-grade. 1 M stock solutions were prepared for each salt in DDI water followed by filtration through a 0.02 µm syringe filter (Whatman, Anotop 25).

Time-resolved dynamic light scattering

Cit-AuNP stability was studied as a function of ionic strength (KCl) in the presence and absence of the 4 NOM isolates at a concentration of 1 mg C/L. In addition, aggregation was quantified in 80 mM KCl at NOM concentrations varying from 0 to 10 mg C/L. In all aggregation studies, the ambient pH after dispersion was between 5 and 6 and cit-AuNP concentrations were 1 mg/L as Au, unless otherwise noted.

Aggregation of the cit-AuNP suspensions was quantified using time-resolved dynamic light scattering (TR-DLS); the intensity-weighted hydrodynamic diameter (D_h) was measured at 15 s intervals for periods ranging from 10-30 min with a 90Plus particle size analyzer (Brookhaven Instruments, Holtsville, NY). Details of the specific procedures have been reported previously.[21] In short, cit-AuNPs were suspended in DDI water in 3.5 mL cuvettes and the size was checked. Then, the NOM isolate was added and the size was checked again. Finally, electrolyte was added and the cuvette was quickly inverted and placed in the instrument.

Aggregation rates were calculated from the initial slope of a plot of D_h vs. t and converted to attachment efficiencies following the procedure outlined by Elimelech and co-workers.[7, 26-28] The initial slope of D_h vs. t is proportional to the absolute aggregation rate coefficient as shown in Eq. 1) [27]:

$$\left(\frac{d(D_h)}{dt}\right)_{t\to 0} \propto k_{11}N_0 \qquad (1)$$

Where k_{11} is the absolute aggregation rate coefficient between primary particles and N_0 is the initial number concentration of primary particles. The attachment efficiency, α, is the aggregation rate constant at a particular condition normalized by the aggregation rate constant in the diffusion-limited (fast) regime as shown in Eq. 2.[26]

$$\alpha = \frac{k_{11}}{k_{11,fast}} = \frac{\frac{1}{N_0}\left(\frac{d(D_h)}{dt}\right)_{t\to 0}}{\frac{1}{N_{0,fast}}\left(\frac{d(D_h)}{dt}\right)_{t\to 0,fast}} \qquad (2)$$

If the initial number concentrations are the same in all aggregation trials, there is no need to calculate the absolute rate constant.

Tabulated data of α vs. ionic strength was used to calculate the critical coagulation concentration (CCC), the electrolyte concentration at which the energy barrier due to electrostatic repulsion between NPs is eliminated by screening of the surface potential by counter-ions in solution.[29] If aggregation behavior follows DLVO theory, particles will aggregate slowly in a reaction-limited regime at low electrolyte concentrations. In this regime, the aggregation rate increases with increasing electrolyte concentration. However, once the CCC is reached (and the energy barrier eliminated), particles aggregate rapidly at a rate that becomes independent of ionic strength (diffusion-limited regime). Experimentally, the CCC is calculated as the electrolyte

Cite this: DOI: 10.1039/c0xx00000x

www.rsc.org/xxxxxx

ARTICLE TYPE

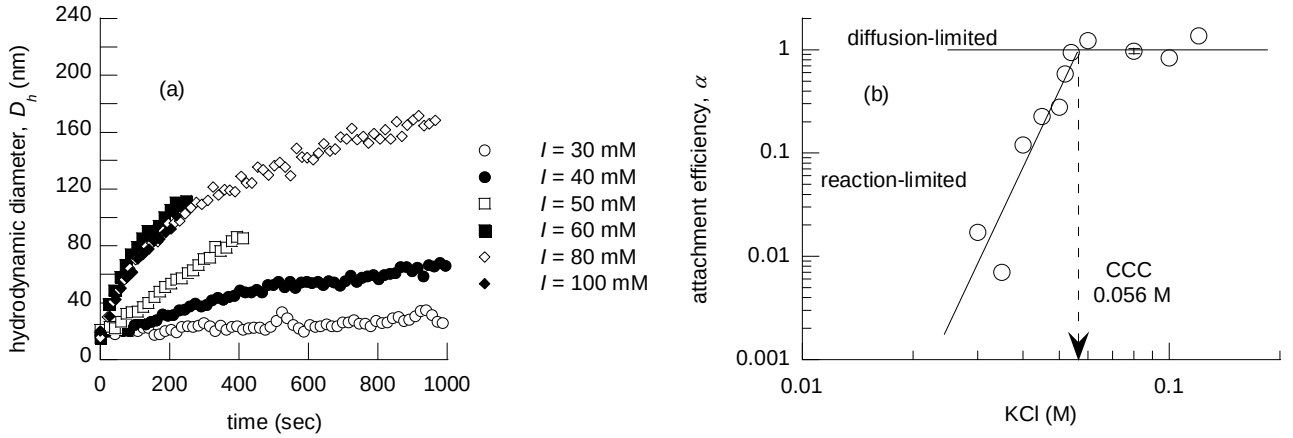

Fig. 1 Aggregation of citrate-stabilized AuNPs in KCl. (a) TR-DLS profiles of Dh for 1 mg/L citrate-stabilized AuNPs in KCl solutions of varying ionic strength. (b) Attachment efficiencies for citrate-stabilized AuNPs as a function of KCl concentration. The CCC calculated from Figure 1b is 56 mM KCl.

concentration where the regression lines extrapolated through the two aggregation regimes intersect. For cit-AuNPs in the presence of the four NOM isolates, initial aggregation rates were converted to attachment efficiencies using the diffusion limited aggregation rate from the cit-AuNPs in KCl without NOM.

Small angle x-ray scattering

Time-resolved small angle x-ray scattering (SAXS) experiments were performed using an Anton Paar SAXSess. cit-AuNP suspensions were prepared in a fixed cuvette as described above and scattering intensity was monitored at 10 s intervals for a period of 1000 s. cit-AuNP concentrations were 10 mg/L for the SAXS trials to achieve suitable scatterin intensities. Scattering data were analyzed using Igor Pro v6.02A software (Wavemetrics, Inc) and the Irena 2 macro[30].

Results and discussion

Ionic strength effects

Aggregation profiles of the cit-AuNPs in varying strength KCl (30-120 mM) are presented in Fig. 1a. In the absence of NOM, the cit-AuNPs exhibit classical DLVO-type behavior. Particles are quite stable at low ionic strengths where a substantial energy barrier exists as a result of electrostatic repulsion between the negatively charged particles (zeta potential = −20 mV at pH = 6 and I = 10 mM[21]). However, as the electrical double layer is compressed by increasing the ionic strength, the rate of aggregation increases until the CCC is reached. Plotting the attachment efficiency against KCl concentration reveals that the critical coagulation concentration is approximately 56 mM KCl (Fig. 1b). These results provide evidence that there is a strong electrostatic component to the stabilization of the AuNPs by the citrate capping agent. Similar results have been reported for the stabilization of TiO_2 NPs by citric acid.[31]

Aggregation data were also collected for 1 mg/L cit-AuNPs suspended in solutions containing KCl (50-450 mM) and 1 mg C/L of each of the four NOM isolates. SRFA and SRHA have been widely used in studies examining NOM effects on colloidal stability and provide a useful point of comparison with previous studies. Only rarely have the effects of these two isolates been compared.[19] SRNOM was chosen to more closely represent NOM character of natural water, but whose effects could also be analysed in reference to its component parts (SRFA and SRHA). SRNOM (as well as SRFA and SRHA) are allocthonous NOM isolates. Finally, PLFA, an autochthonous NOM from a eutrophic lake in Antarctica was chosen because of the contrast in its source and chemical makeup.

Prior to commencing aggregation with the addition of KCl, D_h was measured after equilibration with each NOM isolate as described above. There were no significant differences between the cit-AuNPs in DDI water and the cit-AuNPs in contact with each of the NOM isolates (paired t-tests; α=0.05; n = 10-12 for each condition). These results suggest that if NOM adsorption were taking place at these low ionic strengths, it did not result in a significant change in the initial D_h at the sensitivity detectable by the DLS (95% CIs on the initial diameters ranged from 1.1-3.1 nm).

Aggregation profiles for cit-AuNPs in the presence of the four NOM isolates are shown in Fig. 2. When compared with the results shown in Fig. 1a, Fig. 2a-d reveal that the four NOM isolates stabilized the cit-AuNPs as evidenced by slower rates of aggregation in the presence of NOM at 1 mg C/L, especially at KCl concentrations ranging from 60-100 mM. As with the cit-AuNPs in the absence of NOM, particles are stable at low KCl

Cite this: DOI: 10.1039/c0xx00000x

www.rsc.org/xxxxxx

ARTICLE TYPE

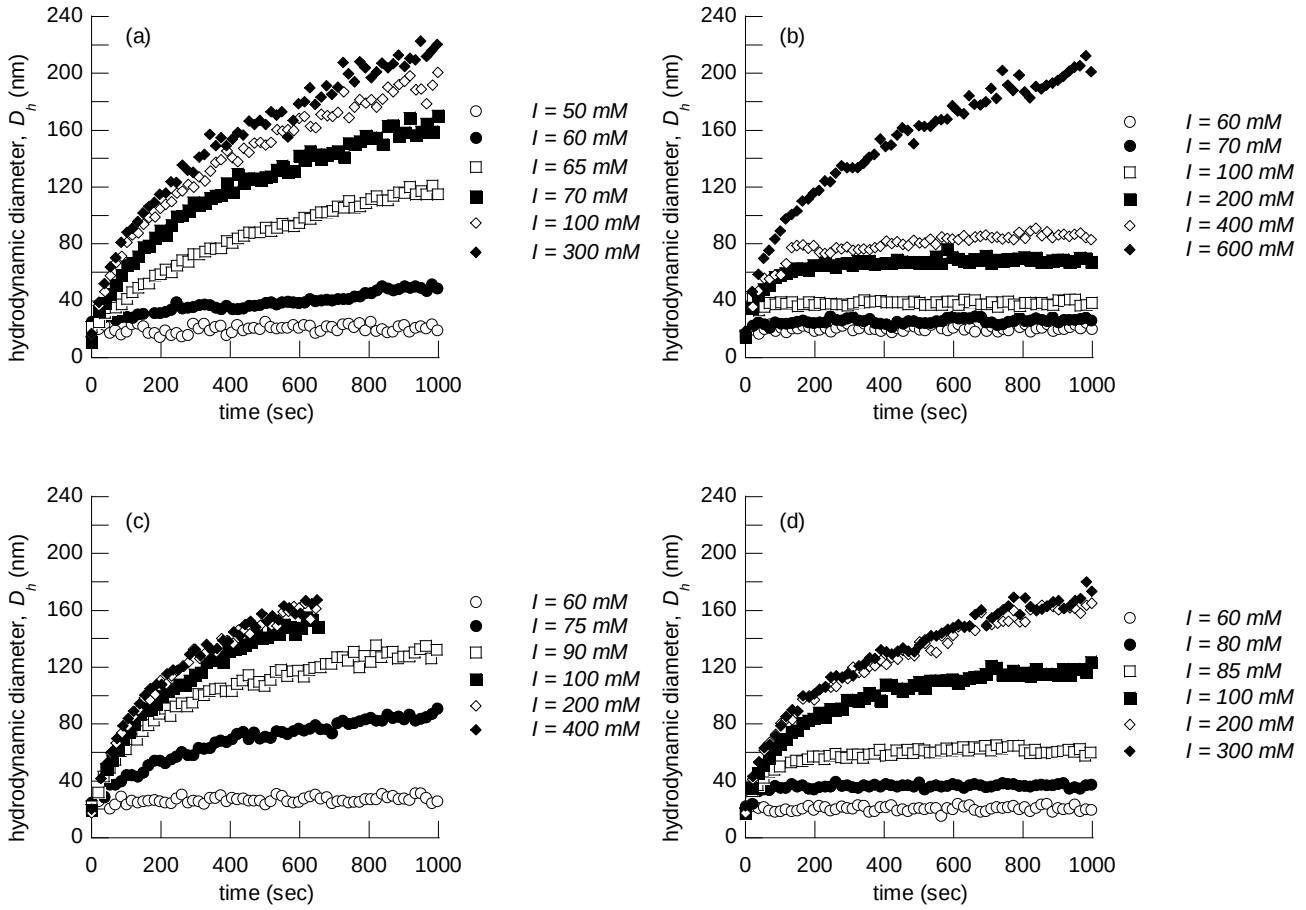

Fig. 2 Aggregation of cit-AuNPs in the presence of NOM isolates and KCl. (a-d) TR-DLS profiles of cit-AuNPs in 1 mg C/L as SRFA, SRHA, SRNOM and PLFA, respectively.

concentrations and aggregation rates increased with increased ionic strength before plateauing.

Attachment efficiencies as a function of KCl concentration are shown in Fig. 3 and the various CCCs are tabulated in the inset. Despite the substantial amount of overlap between the four NOM isolates, it is clear that the CCC for the cit-AuNPs was shifted to higher ionic strengths in the presence of 1 mg C/L as each of the NOM isolates. These results again demonstrate the stabilizing effect of NOM. Furthermore, they indicate that at there is still a strong electrostatic component to the repulsive forces between particles in the presence of the four NOM isolates over the range of ionic strengths investigated. It should be noted that the D_h vs. t profiles of the cit-AuNPs in the presence of SRHA (and to some extent PLFA) were markedly different than for cit-AuNPs in the presence of the other three NOM isolates and calls into question the appropriateness of using a CCC to quantitatively describe aggregation behavior (*vide infra*). Nevertheless, it is clear from Fig. 3 that the cit-AuNPs were stabilized by all four NOM isolates.

Despite similarities in the general trends of NOM-coated AuNP aggregation, the specifics of the aggregation behavior are somewhat different between the four NOM isolates. In the presence of SRFA (Fig. 2a), cit-AuNPs aggregate rapidly at ionic strengths greater than approximately 70 mM. Aggregation is rapid initially and continues at a slowing rate due to the continuous reduction of particle number concentration inherent in all aggregation processes (each NP-NP collision reduces the total number concentration by one).[32] Virtually identical results were seen for SRNOM (Fig. 2c), which is not suprising owing to the fact that SRFA is a primary component of SRNOM.[33]

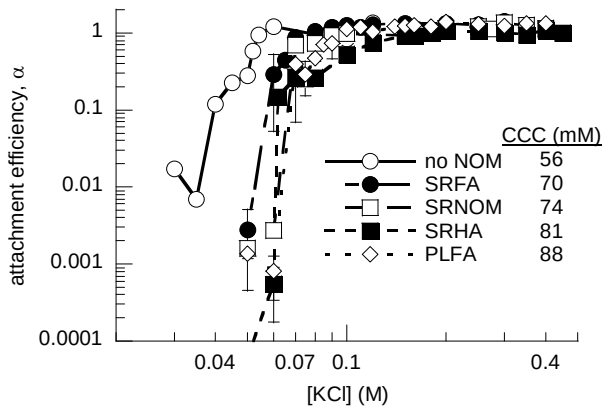

Fig. 3 Attachment efficiencies of AuNPs in the presence of 1 mg C/L of the four NOM isolates. CCC concentrations for AuNPs in each NOM isolate are shown in the inset table.

Comparing the aggregation behavior of cit-AuNPs in the presence of SRFA (Fig. 2a) and SRHA (Fig. 2b) reveal striking differences. Although the D_h of the SRHA coated AuNPs initially increased rapidly at elevated ionic strength, D_h generally leveled off and became relatively stable after approximately 3-5 minutes. For SRHA, D_h did continue to increase after 5 minutes, but at slower rates than the cit-AuNPs in contact with SRFA, which continued to grow rapidly throughout the monitoring period. It wasn't until the ionic strength was increased to > 600 mM KCl that the cit-AuNPs began to aggregate rapidly over the duration of the experiment.

Aggregation profiles for cit-AuNPs in contact with PLFA (Fig. 2d) shared aspects of the characteristics of cit-AuNPs in contact with both SRFA and SRHA. Rates of NP aggregation increased with increasing ionic strength until the CCC was reached, although the CCC was shifted to a higher ionic strength indicating that PFLA is more effective at stabilizing the cit-AuNPs. At ionic strengths ≤120 mM KCl, behavior similar to that of SRHA was seen; profiles were characterized by an initial rapid increase in D_h followed by a relatively stable plateau.

We hypothesize that the the initial change in D_h for cit-AuNPs in contact with SRHA and PLFA is related to changes in NOM conformation or dynamic NOM-AuNP interactions (*e.g.*, adsorption) induced upon the addition of KCl rather than NP-NP aggregation. As has been demonstrated previously, NOM conformation and adsorption to natural colloids and ENPs is strongly influenced by ionic strength. For example, Vermeer *et al.* found that adsorption of purified Aldrich humic acid (AHA) onto hematite nanoparticles increased with increasing ionic strength.[34] This effect was attributed to reduced intramolecular repulsion between adsorbed AHA molecules. Adsorbed layer thicknesses of approximately 40-50 nm were measured by DLS for the particles coated with the large molecular weight AHA. Franchi and O'Melia showed similar results for adsorption of SRHA on latex NPs, documenting 1-4 nm increases in D_h for the 98 nm particles upon addition of 1 mg C/L as SRHA.[9] Again, the findings were attributed to screening of inter- and intramolecular electrostatic forces between functional groups on SRHA molecules at increased ionic strength, resulting in denser adsorbed layers of more highly coiled SRHA molecules that extended further into solution. Recently, Domingos *et al.* attributed increased stability of TiO_2 NPs at increased ionic strength and pH = 8 to increased SRFA adsorption.[8] However, this behavior was not accompanied by a measurable increase in D_h. On the contrary, D_h decreased with increasing ionic strength, a trend that was attributed to increased SRFA adsorption and an accompanying disaggregation of TiO_2 aggregates via steric stabilization.

In context of these previous findings, it is likely that the rapid initial changes in D_h and the influence of ionic strength seen in Figures 2b (≤ 400 mM KCl) and 2d (≤ 120 mM KCl) are the result of increased NOM adsorption rather than NP-NP aggregation. In the case of SRHA, after the short period of adsorption the SRHA coated partcles were quite stable over a range of ionic strengths suggesting that steric stabilization or other non-DLVO interactions were controlling the interaction energy between particles. This was likely also the case for PLFA at ≤ 120 mM KCl. However, in both cases, the repulsive forces were overcome with continued increases in ionic strength. Examining the D_h after approximately 5 minutes in Fig. 2b and 2d suggests that adsorbed layer thicknesses were approximately 4-30 nm for SRHA and 4-12 nm for PLFA. Although increased adsorption with increased ionic strength is also likely occuring for SRFA and SRNOM, these effects are masked by aggregation of the NOM coated cit-AuNPs and are examined further in the section detailing NOM concentration effects.

To begin testing the above hypothesis, we performed preliminary small-angle x-ray scattering experiments in the presence and absence of SRHA in 80 mM KCl. The advantage of SAXS is that it yields direct insitu measurements of nanoparticle core size.[35] In general, these experiments were performed in the same fashion as the TR-DLS experiments. The size of the cit-AuNPs was initially measured and then tracked over time after the addition of KCl. Plots of scattering intensity and fitted size distributions are shown in the supplementary information (Fig. S1-S4†). Initial size measurements of the cit-AuNPs in DDI water revealed a core size of 12.8 nm, very close to the TEM based core size reported by the manufacturer. In the absence of SRHA, significant aggregation of cit-AuNP were detected in the 15 minutes following KCl addition to 80 mM. However, in the presence of SRHA, the cit-AuNP core size was essentially unchanged (12.4 nm) with some minor aggregation detected. These preliminary results support the hypothesis that SRHA inhibits aggregation of cit-AuNPs, but that D_h changes fairly dramatically due to increased adsorption of SRHA molecules onto cit-AuNPs at elevated ionic strength.

As described in the introduction, the use of organic capping agents to stabilize engineered nanoparticles is widespread. Furthermore, much of the research focused on NOM adsorption to colloids and nanoparticles has focused on uncoated inorganic particles. For coated NPs, it is important to understand the interactions between the initial "engineered" coatings and "natural" coatings that result from the adsorption of NOM in natural waters. In previous work we demonstrated, on the basis of electrophoresis measurements, that SRHA adsorbs to AuNPs stabilized by five different organic capping agents. [21] The results reported here support those findings. However, the exact nature

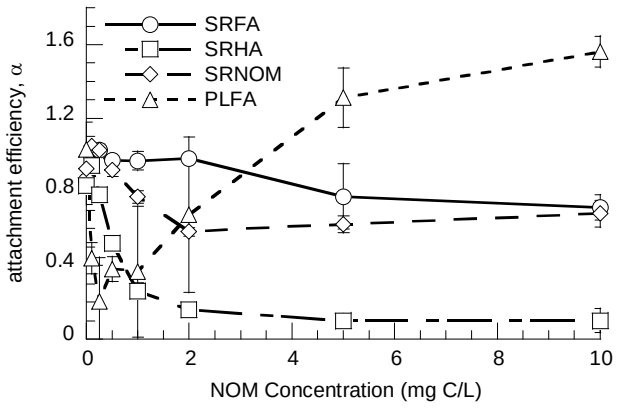

Fig. 4 The influence of NOM concentration of cit-AuNP colloidal stability. Attachment efficiencies as a function of DOC for 1 mg/L cit-AuNPs in 80 mM KCl and varying concentrations (0-10 mg C/L) of each of the four NOM isolates.

of the interactions between NOM and coated AuNPs remains unclear. Citrate molecules have been shown to form inner-sphere complexes with gold[36-38] and TiO_2[31] and likely exist on the surface as the fully deprotonated citrate anion.[39] When placed in contact with other capping agents, citrate can either be replaced[40] or overcoated[41] depending on the competing molecule. Additional work is necessary to determine which method described NOM adsorption to cit-AuNPs.

NOM concentration effects

Differences in aggregation behavior between the cit-AuNPs in contact with the different NOM isolates carried over to the effects of NOM concentration. Fig. 4 details the influence of NOM concentation on the attachment efficiency of AuNPs in the presence of the four NOM isolates in 80 mM KCl. 80 mM was chosen for these trials because at this ionic strength cit-AuNPs are in the diffusion limited regime and (based on the CCC determinations shown in Fig. 3) the presence of NOM would likely provide a moderate degree of stabilization for all four NOM isolates. Raw TRDLS data for each of the four NOM isolates can be found in Figs. S5-S8†.

For cit-AuNPs in the presence of SRFA, it is clear from Fig. 4 that 2-5 mg C/L as SRFA is necessary to significantly influence the colloidal stability of cit-AuNPs. At 5 and 10 mg C/L as SRFA, initial growth rates were roughly 70% of the diffusion limited rates for cit-AuNPs in the absence of NOM. However, after an initial period of rapid increase in D_h, aggregation was much slower (Fig. S5†). In fact, after 5 minutes, aggregation was extremely slow in the presence of 10 mg C/L as SRFA. A D_h of approximately 54 nm was reached after 5 minutes for 10 mg C/L as SRFA, suggesting an adsorbed layer thickness of 21 nm. The behavior of cit-AuNPs in SRFA at 10 mg C/L was very similar to the behavior seen for 1 mg/L SRHA at higher ionic strengths (Fig. 2b). Based on the discussion above, this initial increase in D_h is attributed to increased NOM adsorption rather than NP-NP aggregation.

In contrast to the SRFA results, concentrations of SRHA as low as 0.25 mg C/L increased the stability of the cit-AuNPs in 80 mM KCl. Profiles of D_h vs. t were indicative of SRHA adsorption and subsequent stabilization at concentrations of 0.5 mg C/L and above (Fig. S6†). The influence of SRHA plateaus at approximately 1 mg C/L, suggesting that the adsorption capacity reached a maximum. Unfortunately, it was not possible to corroborate this using standard isotherm techniques due to the limited quantity and relatively high cost of the AuNPs. At concentrations ≥ 1 mg C/L as SRHA there were minimal changes in D_h upon addition of 0.8 mM KCl. Also, the D_h in the presence of 0.5 mg C/L was larger that that at higher NOM concentration, suggesting that perhaps there is some NP aggregation during the initial few minutes when the SRHA is adsorbing to the particles, albeit with a decreased driving force at the lower NOM concentration. This behavior disappears at SRHA concentrations greater than 1 mg C/L, perhaps due to increased adsorption kinetics. The fact that adsorbed layer thicknesses are small is in line with the hypothesis that at low ionic strengths, molecules assume a flat conformation on the NP surface.[9]

The observed differences in the concentration effects for SRFA and SRHA suggest that either SRHA has a higher adsorption capacity on the cit-AuNP surfaces, or that for the adsorption of a fixed amount of NOM, SRHA has a greater influence on NP stability than the same amount of adsorbed SRFA. Such behavior could be related to the differences in physico-chemical properties such as molecular weight or chemical functionality that affect adsorption, or conformation on the NP surface (*vide infra*)

The effect of SRNOM concentration on cit-AuNP agregation was essentially a hybrid between the effects of SRFA and SRHA. In comparison with SRFA, SRNOM began to stabilize NPs at a lower concentration (0.5 mg C/L), consistent with the SRHA results. However, the stabilizing effect appeared to level off at an elevated collision efficiency consistent with the results from the SRFA. At SRNOM concentrations of 5 and 10 mg C/L, AuNPs grew rapidly for the first 3-5 minutes, but were quite stable at D_h = 50-70 nm beyond that point, suggesting adsorbed layer thicknesses of 20-30 nm (Fig. S7†). These results are consistent with the fact that the SRNOM contains both SRHA and SRFA fractions. The fact that the humic fraction is a much smaller percentage of the total would explain both the increased stabilizing effects at lower NOM concentration, as well as the SRFA-like behavior with increasing NOM concentration.

Aggregation of cit-AuNPs in the presence varying concentrations of PLFA was substantially different than for AuNPs in the presence any of the other NOM isolates. Consistent with the CCC results, low concentrations of PLFA (0.1-2 mg C/L) effectively stabilized the cit-AuNPs. However, rapid aggregation occurred in the presence of >2 mg C/L as PLFA. Although the collision efficiency calculations suggest enhanced aggregation, inspection of the raw data (supplementary information) reveal slightly faster initial rates of change of D_h, some of which are likely due to the rapid adsorption/conformational changes described above. After appoximately 5 minutes, the particle sizes in the absence and presence of PLFA (5 and 10 mg C/L) were quite similar (Fig. S8†).

The results at low NOM concentrations are consistent with the results as a function of ionic strength, where PLFA was more

effective at stabilizing the cit-AuNPs than SRFA or SRNOM. The rapid destabilization of particles in the presence of higher concentrations of PLFA could be explained by bridging flocculation induced by favorable interactions between PLFA molecules on adjacent AuNPs that arise at higher surface coverages or when free PLFA molecules remain in solution.[6] As discussed in the introduction, this type of behavior has commonly been seen in solutions containing divalent cations. In this case, with monovalent electrolytes, the behavior could be explained by favorable hydrophobic interactions between PLFA coated particles that occur at increased surface coverages (*vide infra*). Continued efforts are underway to understand the underlying mechanisms.

Correlating AuNP stability with NOM properties

Building on the work of Deonarine *et al*., who recently examined trends in the initial growth rates (combined precipitation and aggregation) of ZnS NPs with various NOM isolates[19], it was our initial hope to correlate CCCs for the four NOM isolates with the physico-chemical properties of the NOM. Because the CCC is theoretically independent of nanoparticle concentration[42] and implicitly incorporates the influence of ionic strength, we believed that it would be a more robust quantitative tool for relating the stabilizing effects of NOM with physico-chemical properties. For example, such relationships have been used to develop structure-property relationships describing the colloidal stability of functionalized carbon nanotubes.[43]

As is clear from the data presented in Fig. 2, it is highly likely that NOM adsorption is also influencing the initial rates of change in D_h. This fact combined with the substantial amount of overlap in the attachment efficiency data in the region of the CCC for the four NOM isolates, the somewhat subjective nature of choosing which data to use to define the diffusion limited regime for purposes of calculating the CCC, and the limited number of NOM isolates resulted in this effort not being fruitful.

Because the NOM isolates investigated in this work are a subset of those used by Deonarine *et al.* we can evaluate the differences in NP stability in the context of that work. For ZnS nanoparticles, the different stabilizing effects of 9 different humic and fulvic acids were attributed primarily to properties related to steric effects; ZnS NPs in the presence of humic substances with higher molecular weight and higher $SUVA_{280}$ consistently had slower growth rates. In a similar analysis, we compared the attachment efficiencies of cit-AuNPs in the presence of 1 mg C/L of each of the NOM isolates in 80 mM KCl (Fig. 4). Under these conditions, stabilizing effects of the four NOM isolates were as follows SRHA > PLFA > SRNOM > SRFA. In general, these trends were evident at other NOM concentrations as well.

SRHA has the highest molecular weight and also the highest aromatic carbon and $SUVA_{280}$ values[19], consistent with the previous work. The fact that SRNOM provide stability intermediate between SRHA and SRFA, but closer to that of SRFA is reasonable based on the fact that SRNOM contains primarily SRFA with a smaller amount of SRHA. However, PLFA, a relatively small fulvic acid with very low aromatic content, provides a substantial amount of stability. Furthermore, PLFA appears to have a greater adsorption density than SRFA at the same ionic strength, and also exhibits a strong destabilizing effect at higher NOM concentrations. PLFA has a much higher alophatic carbon content as well as a higher C:O molar ratio,[19] suggesting that hydrophobic interactions may play an important role in PLFA adsorption and inter-particle interactions.

In general, larger molecular weight NOM isolates appear to provide greater stability and resist destabilization by compression of the electral double layer to a greater extent. However, electrostatic interactions are still important as evidenced by the influence of ionic strength. Clearly the extent of NOM adsorption, the conformation on the NP surface, and the interactions between NOM molecules on adjacent particles are important factors influencing the initial growth rates measured in this work. Efforts are necessary to decouple the NOM adsorption and NP-NP aggregation processes in order to better understand the influence of NOM physico-chemical properties on NP stability.

Summary and Conclusions

As predicted based on the large body of research focused on the stabilizing effect of NOM on natural colloidal stability, it has been shown that four different NOM isolates act to stabilize cit-AuNPs with respect to aggregation. The resulting stability appears to be due to adsorption of the NOM onto the surfaces of the particles although questions remain regarding the nature and mechanisms of these processes. The adsorption process appears to occur over the course of 3-5 minutes upon an increase in ionic strength and is accompanied by NP aggregation in some instances. For the larger molecular weight SRHA at all concentrations and higher concentrations (> 5 mg/L) of lower molecular weight fractions (SRFA and PLFA), it appears that increased NOM adsorption at moderate ionic strengths results in significant increases in the hydrodynamic diameter of the particles, resulting in adsorbed layer thicknesses ranging from 4-30 nm. Preliminary SAXS analysis supports the conjecture that this change in size is not due to NP-NP aggregation. Although the adsorbed NOM layer likely imparts some steric stabilization, ionic strength effects are still evident in the aggregation behavior of NOM-coated AuNPs, suggesting that electrostatic effects remain important.

Despite similarities in the general aggregation trends between the four NOM isolates, each behaved differently in terms of the ionic strength and NOM concentration that resulted in stable NP suspensions. Low concentrations of SRHA and PLFA (≈0.25 mg C/L) were required to induce AuNP stabilization while higher concentrations of SRFA (> 2 mg/L) were required at the same ionic strength. Furthermore, SRNOM, which is largely a mixture of SRHA and SRFA displayed characteristics intermediate between these two fractions with respect to Au-NP stability. At elevated concentrations of PLFA, AuNPs were destabilized, possibly by bridging flocculation induced by favorable hydrophobic interactions between adsorbed PLFA molecules on adjacent NPs.

Clearly, both the type and concentration of NOM, along with the ionic strength of the system are important factors in determining the colloidal stability. Relatively few studies have focused on the influence of NOM type and concentration. We feel these results are a promising first step towards better understanding, and ultimately predicting, NOM-NP interactions and the resulting effects on NP fate and transport. However,

much remains to be done to achieve this goal. Ongoing work is focused on extending these findings to other NOM isolates, other AuNPs with different capping agents and core materials, and incorporating the effects of divalent electrolytes and waters with ionic character simlar to relevant natural waters. Also, we are currently attempting to quantify and characterize NOM adsorption and the nature of the NOM-NP interactions through the use of advanced surface analytical techniques.

Acknowledgements

We thank Howard Fairbrother at Johns Hopkins University for his insightful comments and advice, Sarah Williams and Dylan Stankus at Oregon State University for their contributions to the early portion of this work and Erik Richman at the University of Oregon for assistance with the SAXS analysis. This work was funded by the Air Force Research Laboratory (agreement number FA8650-05-1-5041) and the National Science Foundation (Award 1067794).

Notes

[a] *School of Chemical, Biological and Environmental Engineering, Oregon State University, 103 Gleeson Hall, Corvallis, OR, 97331, USA. Fax: +1 541-737-4600; Tel: +1 541-737-9911; E-mail: jeff.nason@oregonstate.edu*

[b] *School for Engineering of Matter, Transport and Energy, Arizona State University, 501 E. Tyler Mall, Tempe, AZ, USA. E-mail: twcallah@asu.edu*

† Electronic Supplementary Information (ESI) available: Figs. S1-S4 contain SAXS data for cit-AuNPs in the presence and absence of SRHA and Figs. S5-S8 contain TR-DLS data for cit-AuNPs in various concentrations of the 4 NOM isolates. See DOI: 10.1039/b000000x/

‡ *E-mail: mcdowels@onid.orst.edu*

References

1 Woodrow Wilson International Center for Scholars, *The Project on Emerging Nanotechnologies: Nanotechnology Consumer Product Inventory*, http://www.nanotechproject.org/inventories/consumer, Accessed December, 2011, 2011.

2 M. R. Wiesner, G. V. Lowry, P. Alvarez, D. Dionysiou and P. Biswas, *Environmental Science & Technology*, 2006, **40**, 4336-4345.

3 M. R. Wiesner, G. V. Lowry, K. L. Jones, J. M. F. Hochella, R. T. Di Giulio, E. Casman and E. S. Bernhardt, *Environmental Science & Technology*, 2009, **43**, 6458-6462.

4 J. Buffle, K. J. Wilkinson, S. Stoll, M. Filella and J. W. Zhang, *Environmental Science & Technology*, 1998, **32**, 2887-2899.

5 C. L. Tiller and C. R. Omelia, *Colloids and Surfaces a-Physicochemical and Engineering Aspects*, 1993, **73**, 89-102.

6 E. Tipping and D. C. Higgins, *Colloids and Surfaces*, 1982, **5**, 85-92.

7 K. L. Chen and M. Elimelech, *Journal of Colloid and Interface Science*, 2007, **309**, 126-134.

8 R. F. Domingos, N. Tufenkji and K. J. Wilkinson, *Environmental Science & Technology*, 2009, **43**, 1282-1286.

9 A. Franchi and C. O'Melia, *Environmental Science & Technology*, 2003, **37**, 1122-1129.

10 H. Hyung, J. D. Fortner, J. B. Hughes and J.-H. Kim, *Environmental Science & Technology*, 2007, **41**, 179-184.

11 A. A. Keller, H. T. Wang, D. X. Zhou, H. S. Lenihan, G. Cherr, B. J. Cardinale, R. Miller and Z. X. Ji, *Environmental Science & Technology*, 2010, **44**, 1962-1967.

12 Y. Zhang, Y. S. Chen, P. Westerhoff and J. Crittenden, *Water Res*, 2009, **43**, 4249-4257.

13 Y. Zhang, Y. S. Chen, P. Westerhoff, K. Hristovski and J. C. Crittenden, *Water Res*, 2008, **42**, 2204-2212.

14 S. W. Bian, I. A. Mudunkotuwa, T. Rupasinghe and V. H. Grassian, *Langmuir*, 2011, **27**, 6059-6068.

15 A. R. Petosa, D. P. Jaisi, I. R. Quevedo, M. Elimelech and N. Tufenkji, *Environmental Science & Technology*, 2010, **44**, 6532-6549.

16 D. Grasso, K. Subramaniam, M. Butkus, K. Strevett and J. Bergendahl, *Re/Views in Environmental Science and Bio/Technology*, 2002, **1**, 17-38.

17 T. Phenrat, J. E. Song, C. M. Cisneros, D. P. Schoenfelder, R. D. Tilton and G. V. Lowry, *Environmental Science & Technology*, 2010, **44**, 4531-4538.

18 K. Yang, D. Lin and B. Xing, *Langmuir*, 2009, **25**, 3571-3576.

19 A. Deonarine, B. L. T. Lau, G. R. Aiken, J. N. Ryan and H. Hsu-Kim, *Environmental Science & Technology*, 2011, **45**, 3217-3223.

20 K. J. Wilkinson, J.-C. Negre and J. Buffle, *Journal of Contaminant Hydrology*, 1997, **26**, 229-243.

21 D. P. Stankus, S. E. Lohse, J. E. Hutchison and J. A. Nason, *Environmental Science & Technology*, 2011, **45**, 3238-3244.

22 J. Gao, S. Youn, A. Hovsepyan, V. L. Llaneza, Y. Wang, G. Bitton and J. C. J. Bonzongo, *Environmental Science & Technology*, 2009, **43**, 3322-3328.

23 R. D. Holbrook, C. N. Kline and J. J. Filliben, *Environmental Science & Technology*, 2010, **44**, 1386-1391.

24 S. Biggs, P. Mulvaney, C. F. Zukoski and F. Grieser, *Journal of the American Chemical Society*, 1994, **116**, 9150-9157.

25 M. Stobiecka, K. Coopersmith and M. Hepel, *Journal of Colloid and Interface Science*, 2010, **350**, 168-177.

26 K. L. Chen and M. Elimelech, *Langmuir*, 2006, **22**, 10994-11001.

27 K. L. Chen, S. E. Mylon and M. Elimelech, *Environmental Science & Technology*, 2006, **40**, 1516-1523.

28 K. L. Chen, S. E. Mylon and M. Elimelech, *Langmuir*, 2007, **23**, 5920-5928.

29 R. J. Hunter, ed., *Foundations of Colloid Science*, Second edn., Oxford University Press, Inc., New York, NY, 2001.

30 J. Ilavsky and P. R. Jemian, *Journal of Applied Crystallography*, 2009, **42**, 347-353.

31 I. A. Mudunkotuwa and V. H. Grassian, *Journal of the American Chemical Society*, 2010, **132**, 14986-14994.

32 K. L. Chen, B. A. Smith, W. P. Ball and D. H. Fairbrother, *Environmental Chemistry*, 2010, **7**, 10-27.

33 R. L. Malcolm, G. R. Aiken, E. C. Bowles and J. D. Malcolm, in *Humic Substances in the Suwannee River, GA: Interaction, Properties, and Proposed Structures*, eds. R. C. Averett, J. A. Leenheer, D. M. McKnight and K. A. Thorn, USGS, Denver, CO, Editon edn., 1989, vol. Open File Report 87-557, pp. 13-19.

34 A. W. P. Vermeer, W. H. van Riemsdijk and L. K. Koopal, *Langmuir*, 1998, **14**, 2810-2819.

35 L. C. McKenzie, P. M. Haben, S. D. Kevan and J. E. Hutchison, *Journal of Physical Chemistry C*, 2010, **114**, 22055-22063.
36 S. Floate, M. Hosseini, M. R. Arshadi, D. Ritson, K. L. Young and R. J. Nichols, *Journal of Electroanalytical Chemistry*, 2003, **542**, 67-74.
37 Y. Lin, G. B. Pan, G. J. Su, X. H. Fang, L. J. Wan and C. L. Bai, *Langmuir*, 2003, **19**, 10000-10003.
38 R. J. Nichols, I. Burgess, K. L. Young, V. Zamlynny and J. Lipkowski, *Journal of Electroanalytical Chemistry*, 2004, **563**, 33-39.
39 J. Kunze, I. Burgess, R. Nichols, C. Buess-Herman and J. Lipkowski, *Journal of Electroanalytical Chemistry*, 2007, **599**, 147-159.
40 T. Zhu, K. Vasilev, M. Kreiter, S. Mittler and W. Knoll, *Langmuir*, 2003, **19**, 9518-9525.
41 S. H. Brewer, W. R. Glomm, M. C. Johnson, M. K. Knag and S. Franzen, *Langmuir*, 2005, **21**, 9303-9307.
42 H. Holthoff, S. U. Egelhaaf, M. Borkovec, P. Schurtenberger and H. Sticher, *Langmuir*, 1996, **12**, 5541-5549.
43 B. Smith, K. Wepasnick, K. E. Schrote, H. H. Cho, W. P. Ball and D. H. Fairbrother, *Langmuir*, 2009, **25**, 9767-9776.